
Learning Symbolic Rules for Interpretable Deep Reinforcement Learning

Zhihao Ma¹ Yuzheng Zhuang² Paul Weng³ Hankz Hankui Zhuo¹ Dong Li² Wulong Liu² Jianye Hao²

¹School of Computer Science, Sun Yat-Sen University

²Noah's Ark Lab, Huawei

³UM-SJTU Joint Institute, Shanghai Jiao Tong University

Abstract

Recent progress in deep reinforcement learning (DRL) can be largely attributed to the use of neural networks. However, this black-box approach fails to explain the learned policy in a human understandable way. To address this challenge and improve the transparency, we propose a Neural Symbolic Reinforcement Learning framework by introducing symbolic logic into DRL. This framework features a fertilization of reasoning and learning modules, enabling end-to-end learning with prior symbolic knowledge. Moreover, interpretability is achieved by extracting the logical rules learned by the reasoning module in a symbolic rule space. The experimental results show that our framework has better interpretability, along with competing performance in comparison to state-of-the-art approaches.

1 INTRODUCTION

Deep reinforcement learning (DRL) has achieved great success in sequential decision-making problems such as Atari Games [Mnih et al., 2015] and Go [Silver et al., 2017]. However, it is hard to apply DRL to practical problems due notably to its lack of interpretability. Interpretability of DRL is important in earning people's trust and developing a robust and responsible system, especially in applications related to human safety such as autonomous driving. Moreover, an interpretable system makes problems traceable and debugging easier. Therefore, interpretability has attracted increasing attention in the DRL community recently.

Interpretability can be either post-hoc or intrinsic, depending on how it is obtained. For the post-hoc case, the black-box model is explained after training by visualizing for instance t-SNE and saliency maps [Zahavy et al., 2016] or attention masks [Shi et al., 2020b]. For the intrinsic case,

interpretability is entailed by the inherent transparent property of the model [Lipton, 2016]. Our work falls in this case. To improve the interpretability of DRL, we investigate an approach that represents states and actions using first-order logic (FOL) and makes sequential decisions via neural-logic reasoning [Shi et al., 2020a]. In this setting, interpretability is enabled by inspecting the FOL rules used in the action selection, which can be easily understood and examined by a human. A number of algorithms [Jiang and Luo, 2019, Dong et al., 2019, Payani and Fekri, 2020] involving FOL take advantage of neural networks to induce a policy that performs the action selection via approximate reasoning on symbolic states and possibly additional prior knowledge. In this context, an action atom with higher confidence of being true is selected after performing some reasoning steps. The rules used in a policy can be learned using a differentiable version of inductive logic programming (ILP) whose goal is to learn FOL rules to explain observed data. When a neural network is employed to represent the policy, it can be trained to learn the rules and perform reasoning over those rules by forward chaining implemented in the neural network architecture. The main issues with those approaches are their potential high-memory requirements and their computational costs, which limit their applicability. Alternatively, Lyu et al. [2019] propose a hierarchical reinforcement learning (HRL) approach where a high-level (i.e., task level) policy selects tasks which are then solved by low-level (i.e., action level) policies. The low-level policies interact directly with the environment through potential high-dimensional inputs, while the high-level policy makes decisions via classical planning. While this approach can scale to larger problems, it depends on the expert specification of the planning problem to implement the high-level policy.

To alleviate the issues discussed above, we propose a novel framework named Neural Symbolic Reinforcement Learning (NSRL). In this framework, the policy is induced via a neuro-logic reasoning module without any need of predefined oracle rules or transition model specified in advance,

saving expert knowledge dependency compared to Lyu et al. [2019]. In contrast to differentiable ILP methods, NSRL can extract the logical rules selected by the attention modules instead of storing all the rules, thus saving memory budget and improving scalability. To the best of our knowledge, this is the first work introducing reasoning into reinforcement learning (RL) that can succeed in complex domains while remaining interpretable. More specifically, this framework features a reasoning module based on neural attention networks, which performs relational reasoning on symbolic states and induces the RL policy. The proposed framework is evaluated on Montezuma’s Revenge and Blocks World. The experimental results demonstrate competing performance with comparison to state-of-the-art RL approaches while providing improved interpretability by extracting the most relevant relational paths.

2 RELATED WORK

2.1 INDUCTIVE LOGIC PROGRAMMING

Poor generalization ability and interpretability are common in current machine learning algorithms. Inductive logic programming (ILP), an approach aiming to induce logical rules from data, is promising to address the above mentioned limitations [Cropper et al., 2020]. Traditional inductive logic programming approaches require the search in a discrete space of rules and are not robust to noise [Evans and Grefenstette, 2018]. To address those issues, many recent works have proposed various differentiable versions of ILP [Evans and Grefenstette, 2018, Dong et al., 2019, Payani and Fekri, 2020]. However, they are all based on simulating forward chaining and suffer from some form of scalability issues [Yang and Song, 2020]. In contrast, multi-hop reasoning methods [Gardner and Mitchell, 2015, Das et al., 2017, Lao and Cohen, 2010, Yang and Song, 2020] allow answering queries involving two entities over a knowledge graph (KG) by searching a relational path between them. In the ILP context, such paths can be interpreted as grounded first order rules. Interestingly, they can be computed via matrix multiplication [Yang et al., 2017]. Compared to differentiable ILP, multi-hop reasoning methods have demonstrated better scalability. Our work can be seen as the extension of the work by Yang and Song [2020] to the RL setting.

2.2 INTERPRETABLE REINFORCEMENT LEARNING

Recent work on interpretable DRL can be classified into two types of approaches, focusing either on (i) intrinsic interpretability or (ii) post-hoc explanation. Intrinsic interpretability requires the learned model to be self-understandable by nature, which is achieved by using a transparent class of models, whereas post-hoc explanation

entails learning a second model to explain an already-trained black-box model. In type (i) approaches, a (more) interpretable policy can be learned directly online by considering a specific class of interpretable policies (e.g., [Lyu et al., 2019]), or by enforcing interpretability via architectural inductive bias (e.g., [Zambaldi et al., 2018], Jiang and Luo [2019], Dong et al. [2019]). Alternatively, an interpretable policy can also be obtained from a trained one via imitation learning. [Bastani et al., 2018, Verma et al., 2018, Verma, 2019] In type (ii) approaches, various techniques have been proposed to explain the policy of DRL agents using t-SNE and/or saliency maps [Zahavy et al., 2016, Greydanus et al., 2018, Gupta et al., 2019], attention masks [Shi et al., 2020b], visual summaries extracting from histories [Sequeira and Gervasio, 2020], reward decomposition [Juozapaitis et al., 2019], causal model [Madumal et al., 2020], Markov chain [Topin and Veloso, 2019]. More related to interpretable policies, some work in approach (ii) also tries to obtain a more understandable policy [Coppens et al., 2019] in order to explain a trained RL agent. Our work falls in the intrinsic case, which preserves interpretability by learning a set of logical rules described by the First-Order Logic.

3 PRELIMINARY

In this section, we give a brief introduction to the background knowledge necessary for the proposed framework. Interpretable rules described by First-Order Logic are first introduced, then the basics of Reinforcement Learning (RL) are briefly recalled.

3.1 FIRST ORDER LOGIC

A typical First-Order Logic (FOL) system consists of three components: **Entity**, **Predicate** and **Formula**. Entities are constants (e.g., objects) while a predicate can be seen as a relation between entities. An **atom** $\alpha = P(t_1, t_2, \dots, t_n)$ is composed with a n -nary predicate P and n terms $\{t_1, t_2, \dots, t_n\}$, where a term can be a constant or variable. An atom is grounded if all terms in this atom are constants. A **formula** is an expression formed with atoms, logical connectives, and possibly existential and universal quantifiers. In the context of ILP, one is interested to learn formulas of restricted forms called rules. A rule also called **clause** can be written as follows:

$$\alpha \leftarrow \alpha_1 \wedge \alpha_2, \dots, \wedge \alpha_n$$

where α is called *head atom* and $\alpha_1, \alpha_2, \dots, \alpha_n$ are called *body atoms*. A clause is grounded with all the associated atoms grounded. The head atom is believed to be true only if all the body atoms are true. For example, $Connected(X, Z) \leftarrow Edge(X, Y) \wedge Edge(Y, Z)$ is a clause where X, Y, Z are variables and $Connected, Edge$ are predicates. If we substitute X, Y, Z with constants a, b, c , then a and c are considered connected if $Edge(a, b)$ and $Edge(b, c)$

hold. Embedded with prior knowledge, clauses described by FOL are highly understandable and interpretable. Following most previous neural symbolic approaches, function symbols and recursive definitions are not considered in this work.

3.2 REINFORCEMENT LEARNING

Consider a Markov Decision Process defined by a tuple $(S, A, P_{ss'}^a, r_s^a, \gamma)$ where S and A denote the state space and action space, respectively, $P_{ss'}^a$ provides the transition probability of moving from state $s \in S$ to state $s' \in S$ after taking action $a \in A$, r_s^a is the immediate reward obtained after performing action a in state s and $\gamma \in [0, 1]$ is a discount factor. The objective of an RL algorithm is to find a deterministic policy $\pi : S \rightarrow A$ or a stochastic policy $\pi : S \rightarrow \Delta(A)$ (with $\Delta(A)$ being the set of probability distributions over A) that maximizes the expected return $V_\pi(s) = \mathbb{E}_\pi[\sum_{t=0}^{\infty} \gamma^t r_t \mid s_0 = s]$ where r_t is the reward at time step t received by following π from state $s_0 = s$. The state-action value function is defined as follows: $Q_\pi(s, a) = \mathbb{E}_\pi[\sum_{t=0}^{\infty} \gamma^t r_t \mid s_0 = s, a_0 = a]$.

4 NEURAL SYMBOLIC REINFORCEMENT LEARNING

In this section, we first explain the overall structure of our architecture called Neural Symbolic Reinforcement Learning (NSRL), including the fertilization of three components, i.e., reasoning module, attention module, and policy module. After that, we describe these three components in detail, and present the training process of our NSRL approach.

4.1 SYSTEM FRAMEWORK

In this section, we describe the structure of NSRL. As shown in Figure 1, the symbolic states from the environment are firstly transformed into a matrix \mathbf{P} , of which each row represents a specific predicate. This matrix is then sent to the attention module composed of the predicate and path attention submodules. The predicate attention submodule iteratively processes matrix \mathbf{P} resulting in the generated attention weights $\mathbf{S}_\varphi = (s_\varphi^{(1)}, \dots, s_\varphi^{(T)})$ on predicates at each reasoning step, where T is the maximum number of reasoning steps. Then, the outputs at each step from the predicate attention submodule are concatenated and sent to the path attention submodule to produce attention weights $\mathbf{S}_\psi = (s_\psi^{(1)}, \dots, s_\psi^{(T)})$ on logical rules of different length. Next, matrix \mathbf{P} and the attention weights are sent to the reasoning module to perform reasoning on existing symbolic knowledge. As illustrated in the right part of Figure 1, each column of \mathbf{S}_φ represents the attention weights on predicates at a reasoning step. Assuming that $T = 4$, we denote the predicate matrix at each step as $\mathbf{P}^{(1)}, \mathbf{P}^{(2)}, \mathbf{P}^{(3)}, \mathbf{P}^{(4)}$, which are the results of the multiplica-

tion of \mathbf{S}_φ and the symbolic matrix \mathbf{P} . Then, we sequentially multiply these matrices to generate logical rules of different lengths. Next, we apply path attention weights \mathbf{S}_ψ on these rules to generate the reasoning results. These results are then sent to the multi-layer perceptrons (MLP) in the policy module. Each branch of the MLP output corresponds to an action predicate. In the figure, we assume that there are in total m action predicates: $A_1, A_2, A_3, \dots, A_m$. In the end, we can choose the action atom based on the value of these action predicate matrices.

4.2 REASONING MODULE

Consider a knowledge graph, where objects are represented as nodes and relations are edges. Multi-hop reasoning on such a graph mainly focuses on searching chain-like logical rules of the following form:

$$query(x, x') \leftarrow R_1(x, z_1) \wedge R_2(z_1, z_2) \cdots \wedge R_n(z_{n-1}, x'). \quad (1)$$

The task of multi-hop reasoning for a given query corresponds to finding a relational path from x to x' with multi-steps $x \xrightarrow{R_1} \dots \xrightarrow{R_n} x'$. Based on Yang et al. [2017], the inference of this logical path can be seen as a process of matrix multiplication. Every predicate or relation P_k is represented as a binary matrix \mathbf{M}_k in $\{0, 1\}^{|\mathcal{X}| \times |\mathcal{X}|}$, whose entry (i, j) is 1 if $P_k(x_i, x_j)$ holds, i.e., entity x_i and x_j are connected by edge P_k in the knowledge graph. Set \mathcal{X} contains the objects of the problem. Let \mathbf{v}_x denote the one-hot encoding of an object x . Then, the t -th hop of the reasoning along the path can be computed as:

$$\mathbf{v}^{(0)} = \mathbf{v}_x, \quad (2)$$

$$\mathbf{v}^{(t)} = \mathbf{M}^{(t)} \mathbf{v}^{(t-1)}, \quad (3)$$

where $\mathbf{M}^{(t)}$ is the matrix used in t -th hop and $\mathbf{v}^{(t-1)}$ is the path feature vector. After T steps reasoning, the score of the query for one path is computed as follows:

$$score(x, x') = \mathbf{v}_x^T \prod_{t=1}^T \mathbf{M}^{(t)} \cdot \mathbf{v}_{x'}, \quad (4)$$

Considering all the predicate matrices at each step and relational paths of different lengths, the final score can be rewritten with soft attention as below:

$$\kappa(\mathbf{S}_\psi, \mathbf{S}_\varphi) = \sum_{t'=1}^T s_\psi^{(t')} \left(\prod_{t=1}^{t'} \sum_{k=1}^N s_{\varphi,k}^{(t)} \mathbf{M}_k \right), \quad (5)$$

$$score(x, x') = \mathbf{v}_x^T \kappa(\mathbf{S}_\psi, \mathbf{S}_\varphi) \mathbf{v}_{x'}, \quad (6)$$

where T is the maximum reasoning steps, $\mathbf{S}_\psi = (s_\psi^{(t)})_{t'}$, $\mathbf{S}_\varphi = (s_{\varphi,k}^{(t)})_{t,k}$, term $s_\psi^{(t')}$ corresponds to attention weights over relational paths of length t' , and $s_{\varphi,k}^{(t)}$ to another attention weights on predicate matrix \mathbf{M}_k used in the t -th step, and N denotes the total number of predefined predicates.

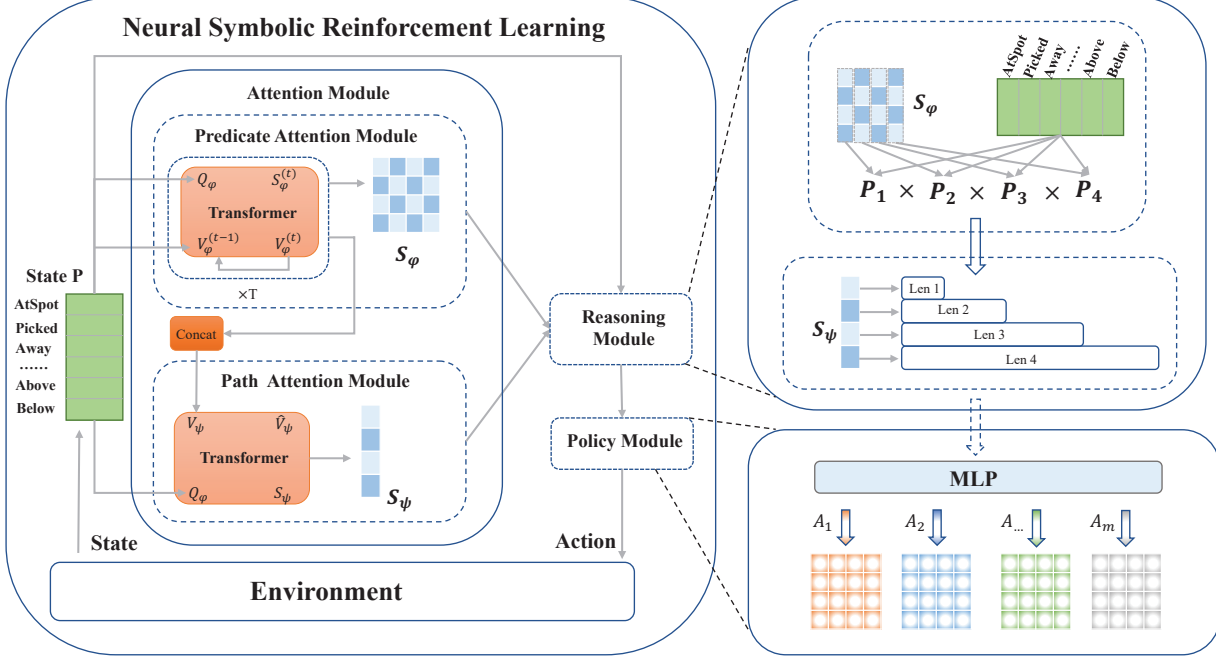


Figure 1: System framework of NSRL. The left part illustrates the three major components of NSRL, i.e., reasoning module, attention module, and policy module, which are described in Section 4.2, Section 4.3, and Section 4.4, respectively. The right part details the reasoning module and policy module.

4.3 ATTENTION MODULE

In this section, we introduce the architecture of the attention module, a hierarchical stack of transformers, to generate the dynamic attention weights. Recall a basic multi-head dot-product attention module (MHDPA) in the transformer architecture [Vaswani et al., 2017] takes as inputs the query, key and value representations: \mathbf{Q} , \mathbf{K} , \mathbf{V} . MHDPA firstly computes the similarity or attention weights \mathbf{S} between the query and the key, and then calculates the weighted value as output \mathbf{V}' :

$$\text{MHDPA}(\mathbf{Q}, \mathbf{K}, \mathbf{V}) = \mathbf{S}, \mathbf{V}' \quad (7)$$

$$\text{with } \mathbf{S} = \text{softmax}\left(\frac{\mathbf{Q}\mathbf{K}^\top}{\sqrt{d}}\right) \text{ and } \mathbf{V}' = \mathbf{S}\mathbf{V}, \quad (8)$$

where d is the dimension of \mathbf{K} .

We utilize this module to generate the attention weights \mathbf{S}_ϕ and \mathbf{S}_ψ . In fact, the symbolic states can be represented as a 3-dimensional tensor $\mathbf{M} \in [0, 1]^{|\mathcal{X}| \times |\mathcal{X}| \times N}$, where \mathcal{X} denotes the set of extracted objects and N represents the numbers of predefined predicates. We transform tensor \mathbf{M} into a matrix $\mathbf{M}_f \in [0, 1]^{|\mathcal{X}|^2 \times N}$ at each time step. Each row of matrix \mathbf{M}_f represents a part of the symbolic state, which can be seen as an embedding of predicate. In this way, the attention module can generate weights on predicates at different reasoning steps, taking consideration of the symbolic information of

current RL state. We firstly generate the query, key and value representations with multi-layer perceptrons with \mathbf{M}_f as initial input. For convenience, we define $\mathbf{V}_\phi^{(0)} = \mathbf{M}_f$. Then, we repeatedly use the output value from last step to generate the attention weights. The predicate attention submodule can be summarized as follows:

$$\mathbf{Q}_\phi^{(t)}, \mathbf{K}_\phi^{(t)}, \mathbf{V}_\phi^{(t)} = \text{FeedForward}_t(\mathbf{V}_\phi^{(t-1)}), \quad (9)$$

$$\mathbf{s}_\phi^{(t)}, \mathbf{V}_\phi^{(t+1)} = \text{MHDPA}(\mathbf{Q}_\phi^{(t)}, \mathbf{K}_\phi^{(t)}, \mathbf{V}_\phi^{(t)}), \quad (10)$$

where the superscript denotes the reasoning step. Here, $\mathbf{s}_\phi^{(t)}$ represents the attention weights over predicates in the t -th hop reasoning and FeedForward means multi-perceptron layer. For the path attention submodule, we reuse the output value of each time step in the predicate attention submodule. During the iterative processing, the output value at each step embeds the information of paths of different lengths. We simply use another transformer to generate the path attention weights \mathbf{S}_ψ . Let $\mathbf{V}_\psi = [\mathbf{V}_\phi^{(0)}, \mathbf{V}_\phi^{(1)}, \dots, \mathbf{V}_\phi^{(t)}]^\top$.

$$\mathbf{Q}_\psi, \mathbf{K}_\psi, \mathbf{V}_\psi = \text{FeedForward}(\mathbf{V}_\psi), \quad (11)$$

$$\mathbf{S}_\psi, \mathbf{V}'_\psi = \text{MHDPA}(\mathbf{Q}_\psi, \mathbf{K}_\psi, \mathbf{V}_\psi), \quad (12)$$

4.4 POLICY MODULE

In this section, we build a policy module for generating DRL policies. We denote an object set and a predicate set by \mathcal{X}

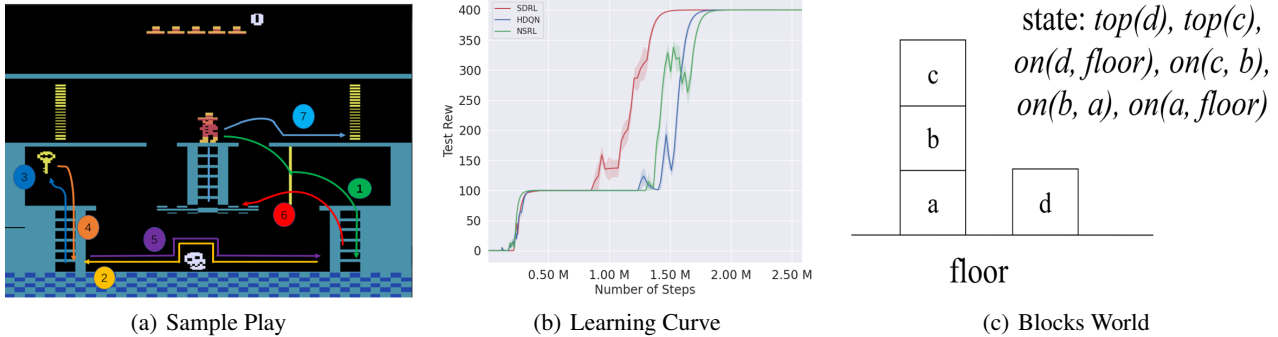


Figure 2: (a) describes the optimal policy learnt by the agents. (b) illustrates the evaluating phase of SDRL, HDQN and NSRL. (c) depicts a sample of the block world domain with the state represented by FOL.

and \mathcal{P} respectively. A predicate set is composed of both action predicates representing the fact of changing states, denoted by \mathcal{P}_a , and state predicates representing the fact of states, denoted by \mathcal{P}_s . Let x and x' represent two entities from \mathcal{X} . We denote an action atom by $Act_a(x, x')$ where Act_a is an action predicate from \mathcal{P}_a . Assuming there exists an oracle capable of extracting symbolic states at each time step, we can represent state and action with FOL. Since a policy is a mapping from states to actions, a predicate at the last hop needs to be constrained to be an action predicate. For every action predicate Act_a , we introduce a multi-layer perceptron MLP_a to the output of the reasoning module to induce the state-action value of action atom $Act_a(x, x')$:

$$Q(S, Act_a(x, x')) = (\mathbf{v}_x^\top MLP_a(\kappa(\mathcal{S}_\psi, \mathcal{S}_\phi)) \mathbf{v}_{x'}), \quad (13)$$

In the context of FOL, we only consider finite action space. To learn a deterministic policy, we update the policy module by minimizing the loss function described below where D is a replay buffer.

$$L(\theta) = \mathbb{E}_{(s, \hat{a}, r, s') \sim D} \left[\left(r + \gamma \max_{\hat{a}'} Q(s', \hat{a}'; \theta) - Q(s, \hat{a}; \theta) \right)^2 \right],$$

where \hat{a} and \hat{a}' denote action atoms. To learn a stochastic policy, we use the *softmax* function on the state-action values and obtain probabilities over taking action atoms. Then, we can train NSRL with any deep RL algorithms such as DQN [Mnih et al., 2015] or policy gradient methods (e.g., REINFORCE [Williams, 1992], PPO [Schulman et al., 2017]).

5 EXPERIMENTS

In this section, we evaluate our approach on two domains, i.e., Montezuma's Revenge and Blocks World Manipulation, in terms of expected returns, generalization ability, and interpretability. We measure the performance of our approach in terms of expected returns. Higher returns indicate better performance. To validate the generalization ability leveraged by symbol logic, we compute the expected returns the

agents receive in unseen environments. We qualify a method as interpretable if it can present the logical rules learned in the training process. We compare our proposition with relevant state-of-the-art algorithms in both domains. We set the learning rate to be $1e-4$, the maximum reasoning steps to be 4 and the number of layers and heads in the attention module to be 2 and 4 separately. We describe each domain, the evaluation protocol, and the results next.

5.1 MONTEZUMA'S REVENGE

We first evaluate our approach on *Montezuma's Revenge*, an ATARI game with sparse, delayed rewards, which is also used by Kulkarni et al. [2016]. In this game, the player navigates through several rooms in order to collect treasures. We conduct our experiment based on the first room shown in Figure 2(a). In this room, the player needs to first fetch a key, then navigate to the right door and pass through it. If the player successfully fetches the key, she receives a reward (+100). If she successfully navigates to the door and passes through it, she receives another reward (+300).

5.1.1 Symbolic Representation

The symbolic domain knowledge we use is based on 6 pre-defined locations: *middle ladder*, *(right) door*, *left of rotating skulls*, *lower left ladder*, *lower right ladder* and *key*. One mobile object, the *man* in red, is also introduced. We introduce 6 predicates: **AtSpot**, **WithObject**, **WithoutObject**, **PathExist**, **KeyToDoor** and an action predicate **Move**. Atom **AtSpot**(x, y) means object x is currently at location y . **WithObject**(x, y) means object x possesses object y and **WithoutObject**(x, y) is the opposite. **PathExist**(x, y) means a path from location x to location y exists and **KeyToDoor**(*key*, *door*) means possessing a key is the precondition to open a door. **Move**(x, y) means move object x to location y . To represent a state with the symbolic predicates and objects defined above, we assume there is a pre-trained

oracle capable of answering queries whether a specific atom is true given high-dimensional images as input.

5.1.2 Setup

We compare our approach with HDQN [Kulkarni et al., 2016] and SDRL [Lyu et al., 2019] as baselines. We implement our architecture NSRL and HDQN with an option-based hierarchical reinforcement learning framework similar to SDRL. This framework is split into two levels, meta controller (high level) and action controller (low level). The meta controller assigns a task to be achieved by the action controller. The only difference between these agents is the way to induce a policy in the high level. SDRL requires a symbolic transition model (expert knowledge) and a planner to induce an option trace. HDQN utilizes an end-to-end neural network to induce the higher level policy while NSRL performs neuro-symbolic reasoning. In terms of the low level, all the agents reuse the controller architecture in Kulkarni et al. [2016] and we set the maximum interaction length to be 500. To facilitate the learning process, we define the reward function below for training and use the original reward setting described in Section 5.1 for testing. The controller receives a reward of -0.1 at every step and +10 when achieving the assigned goal. If the controller fails the game or lose its life, it will receive another reward -5. The meta controller will receive -0.5 reward after each decision. We jointly train the two levels of these algorithms with the Deep Double Q-Learning algorithm [Van Hasselt et al., 2016] and prioritized replay buffer [Schaul et al., 2015].

5.1.3 Results

We present the optimal policy learned as shown in Figure 2(a). These agents sequentially learn Tasks 1 to 3 to get +100 reward and explore other Tasks 4 to 7 and finally converge to +400 reward. We estimate expected returns from 8 runs and present the results in Figure 2(b). The performance of these approaches are similar. It takes nearly 1.5M steps for SDRL to converge to the optimal performance (+400 reward) while 1.8M steps are needed for NSRL and HDQN. Due to the use of the ϵ -greedy exploration strategy in Deep Double Q-learning, both NSRL and HDQN take another 0.3M steps on exploration than the planner-based method SDRL. The use of a symbolic planner with the formalization of the planning problem guides the learning agent to induce an increasingly better plan, explaining the faster convergence of SDRL. However, NSRL still performs competitively and similarly to the model-free method HDQN. Both of them start to explore how to fetch a key (+100 reward) and open a door (+400 reward) nearly at the same time. By design, SDRL can provide an interpretable plan. However, we argue that this approach does not scale, since SDRL requires a full description of the planning problem. To compare the dependency on expert knowledge, we enumerate in Table 1

Table 1: Comparison of the three agents in terms of expert knowledge dependency

Method	Expert Knowledge
NSRL	6 locations, 6 predicates
SDRL	6 locations, 5 predicates, 1 transition model
HDQN	—

the symbolic knowledge used in each method. Obviously HDQN does not use any domain knowledge and thus prevents any interpretability with logical rules. Although NSRL uses one extra predicate compared to SDRL, NSRL depends less on expert knowledge than SDRL since designing a symbolic transition model in complicated environments is much harder than predicates. Therefore, it is easier for NSRL to scale to more complex problems than SDRL. We leave the discussion about the interpretability of NSRL to Section 5.3.

5.2 WORLD MANIPULATION

We validate the generalization ability of NSRL in the Blocks Manipulation Environment used by Jiang and Luo [2019]. In this environment, the agent is required to finish three tasks: *STACK*, *UNSTACK* and *ON*. In the *STACK* task, the blocks need to be stacked into a column while they need to be put on the floor in the *UNSTACK* task. In the *ON* task, a specific block is required to be put on another one. In all the tasks, the agents is trained with only 4 blocks while tested with 5 or even more blocks. Three predicates (i.e., **On**, **Top**, and an action predicate **Move**) are used to represent the symbolic states and actions. Another predicate **GoalOn** is also introduced in task *ON* to specify the goal, i.e., **GoalOn(a,b)** means that block *a* should be moved on entity *b*, which can be a block or the floor. Figure 2(c) shows the state $((a,b,c), (d))$ and its symbolic representation.

5.2.1 Setup

The settings of the environments are the same as in [Jiang and Luo, 2019]. In total, there are a maximum of 7 blocks labeled as (a, b, c, d, e, f, g) and one entity labeled as *floor*. The agent is asked to operate on these entities to finish the tasks. In the interaction process, the agent receives a reward of -0.02 at every step and gets a reward of 1 after finishing its task and the maximum length of interaction is set to be 50. If the action is invalid like **Move(floor,a)**, the state will not be changed. In order to test the generalization ability, the agent is trained in environments with 4 blocks while tested in environments with more than 4 blocks. In the *UNSTACK* task, the agent is trained with a single column of blocks like $((a, b, c, d))$. We swap the top 2 blocks or divide the blocks into 2 columns for testing. For the *STACK* task, the initial state is like $((a),(b),(c),(d))$ in the training

Table 2: Expected returns of different agents in training/test environments. The first row provides each agent’s category. The first 2 columns list the tasks and their instances. The next 5 show the performance of the agents, in addition to the optimal returns computed by value iteration (VI).

Type		Rules Learning	Rules Given	No Rules	No Rules	
Method		NSRL	NLRL	NLM	MLP	VI
UNSTACK	training	0.939 ± 0.004	0.935 ± 0.011	-0.773 ± 0.495	0.934 ± 0.012	0.940
	swap top 2	0.939 ± 0.005	0.935 ± 0.010	-0.777 ± 0.492	0.920 ± 0.025	0.940
	2 columns	0.960 ± 0.000	0.956 ± 0.009	-0.424 ± 0.749	-0.951 ± 0.203	0.960
	5 blocks	0.919 ± 0.005	0.910 ± 0.016	-0.953 ± 0.183	0.900 ± 0.256	0.920
	6 blocks	0.894 ± 0.017	0.884 ± 0.020	-0.979 ± 0.044	0.862 ± 0.033	0.900
	7 blocks	0.864 ± 0.020	0.855 ± 0.026	-0.980 ± 0.000	0.762 ± 0.098	0.880
STACK	training	0.940 ± 0.003	0.889 ± 0.046	0.129 ± 0.702	0.937 ± 0.009	0.940
	swap right 2	0.940 ± 0.004	0.889 ± 0.045	0.156 ± 0.688	0.937 ± 0.010	0.940
	2 columns	0.939 ± 0.028	0.919 ± 0.055	0.182 ± 0.709	-0.980 ± 0.000	0.940
	5 blocks	0.917 ± 0.017	0.863 ± 0.053	-0.437 ± 0.699	-0.980 ± 0.000	0.920
	6 blocks	0.878 ± 0.139	0.834 ± 0.069	-0.772 ± 0.491	-0.980 ± 0.000	0.900
	7 blocks	0.826 ± 0.210	0.791 ± 0.134	-0.912 ± 0.286	-0.923 ± 0.257	0.880
ON	training	0.917 ± 0.008	0.913 ± 0.012	-0.823 ± 0.432	0.512 ± 0.468	0.920
	swap top 2	0.907 ± 0.018	0.915 ± 0.010	-0.817 ± 0.437	0.840 ± 0.067	0.920
	swap mid 2	0.916 ± 0.009	0.915 ± 0.011	-0.859 ± 0.383	0.663 ± 0.239	0.920
	5 blocks	0.888 ± 0.018	0.888 ± 0.018	-0.939 ± 0.231	-0.910 ± 0.303	0.900
	6 blocks	0.852 ± 0.030	0.866 ± 0.020	-0.977 ± 0.063	-0.980 ± 0.000	0.880
	7 blocks	0.798 ± 0.048	0.839 ± 0.019	-0.980 ± 0.000	-0.980 ± 0.000	0.860

environment while $((a), (b), (d), (c))$ and $((a, b), (d, c))$ are used in generalization tests. For the *ON* task, the initial state in the training environment is $((a, b, c, d))$ and the goal is to put block a on block b . We also swap the top 2 blocks or middle 2 blocks for testing. Besides, we randomly choose 4 blocks from the total 7 blocks to replace the above mentioned blocks in the training environments and produce more training cases. In all the tasks, the agent is required to test in unseen environment with 5 ~ 7 blocks. The test environments with over 4 blocks are the same in the *UNSTACK* and *ON* tasks, which are $((a, b, c, d, e))$, $((a, b, c, d, e, f))$, and $((a, b, c, d, e, f, g))$. The initial states in test environments with more than 4 blocks for the *STACK* task are $((a), (b), (c), (d), (e))$, $((a), (b), (c), (d), (e), (f))$ and $((a), (b), (c), (d), (e), (f), (g))$. We compare NSRL with NLRL [Jiang and Luo, 2019], NLM [Dong et al., 2019], and a Multi-Layer Perceptron (MLP) in these tasks. NLRL requires rule templates to generate possible rules but NLM and MLP do not allow the extraction of rules after learning. For this reason, we classify these algorithms into three types: Rules Learning, Rules Given and No Rules. The MLP agent has 2 hidden layers with 20 units using RELU [Nair and Hinton, 2010] activation functions. Following NLRL, we train MLP, and NSRL with the PPO algorithm [Schulman et al., 2017] and use generalized advantages ($\lambda = 0.95$) [Schulman et al., 2015]. For the three architectures, we use the same critic network consisting of one 20-unit hidden layer.

Table 3: Comparison of the four agents in terms of inference time and memory cost.

Method	NSRL	NLRL	NLM	MLP
Inference Time (h)	1.219	5.421	1.396	0.168
Memory Cost (GB)	2.715	7.340	2.056	2.682

5.2.2 Results

We exhibit the averages and standard deviations over 1000 repeated evaluations of the three blocks world manipulation tasks in Table 2. We employ a stochastic policy for all the agents in the evaluation phase. From Table 2, we can see that the MLP agent achieves near-optimal performance in the training environments of *UNSTACK* and *STACK* task. However, without any design of logic reasoning in more difficult and complex tasks, the MLP agent fails in most of the testing environments of *STACK* and *ON* task. Although NLM introduces a logical architecture inductive bias, it performs worse than MLP. In general, NLRL outperforms NLM and MLP in terms of expected returns in the three tasks. The logical rules of higher confidence learned from a given rule set in the training environment can be directly reused in the test environments, contributing to its great generalization ability in unseen environments. Besides, NSRL achieves competitive performance compared to NLRL not

Table 4: Logical Rules extracted from NSRL.

Domain	Logical rules
Blocks World	1. $Move(X, Y) \leftarrow GoalOn(X, Y)$ 2. $Move(X, Z) \leftarrow Top(X, X) \wedge On(X, Y) \wedge On(Y, Z)$ 3. $Move(X, M) \leftarrow On(X, Y) \wedge On(Y, Z) \wedge On(Z, M)$ 4. $Move(X, Y) \leftarrow Top(X, X) \wedge GoalOn(X, Y) \wedge Top(Y, Y)$ 5. $Move(X, Z) \leftarrow On(X, Y) \wedge GoalOn(Y, X) \wedge On(X, Y) \wedge On(Y, Z)$
Montezuma’s Revenge	6. $Move(man, key) \leftarrow WithoutObject(man, key)$ 7. $Move(man, door) \leftarrow WithObject(man, key) \wedge KeyToDoor(key, door)$

only in training but also in test environments. In task *UNSTACK*, NSRL achieves near-optimal performance, about 0.05 returns higher than NLRL in training environments and 0.1 higher in test environments. NSRL performs more stably than NLRL. The standard deviations of NSRL is about 0.005 less than NLRL. In the difficult task *STACK*, NSRL achieves the optimal returns in training environment. The performances of both NSRL and NLRL decrease gradually in environments with increasing number of blocks. However, NSRL can still achieve 0.917, 0.878 and 0.826 average returns in environments with 5, 6, and 7 blocks separately, about 0.03 higher than NLRL. In the first four environments of task *ON*, NSRL performs closely to NLRL with the gap between the returns being less than 0.008 and the standard deviations less than 0.005. However in the remaining tests, NLRL performs better.

To compare the scalability between these agents, we evaluate the computation inference time and memory cost for each task averaged over 1000 tests. Although the MLP agent uses least inference time, it performs badly in the test environments and so as the NLM agent. Table 3 illustrates that NSRL scales better than NLRL. Indeed, NLRL takes almost 2.7 times more memory and 4.5 times more inference time than NSRL. The high memory requirement of NLRL, increasing exponentially with the number of predicates, prevents it to scale to a complex domain like Montezuma’s Revenge. These results illustrate that NSRL, without human-designed rules, can also achieve competitive performance with improved scalability. Although NLM uses a symbolic representation, it can not extract logical rules and neither can the MLP agent. Therefore, the policies learned by these two agents are lack of interpretability. The logical rules of higher confidence in NLRL are generated from human designed rules templates and thus are highly interpretable. We leave the discussion about the interpretability of NSRL in the Blocks World domain to the next section.

5.3 INTERPRETABLE POLICY

In this section, we present the logical rules learned by NSRL in the domain of Montezuma’s Revenge and Blocks World Manipulation. We visualize the attention weights for every

predicates at each reasoning step and for paths of different lengths. Then, we multiply these predicate attention weights sequentially. The results of the product are multiplied by the attention weights of the path of the corresponding length. We interpret these results as the confidence of the corresponding logical rules. Since NSRL can only learn chain-like rules, we manually select some of the chain-like logical rules of highest attention weights as shown in Table 4. For example, in the *ON* task, if the current state satisfies rules 1 or 4, it is most likely to take action $Move(X, Y)$. In the Atari Game, a likely reason to choose to get the key as a task is when the agent does not have it. The predicate **KeyToDoor** that we introduced to embed the knowledge that a key is important to open a door also improves the interpretability of the learned rules, i.e., rule 7, which chooses a door as a task. These extracted logical rules are not always true and need to be selected by a human but they do provide a certain interpretation for why an action is chosen. In any case, NSRL is arguably more interpretable than MLP and NLM. NSRL provides a novel way to generate chain-like rules without human designed templates, improving flexibility and saving human labour.

6 CONCLUSION

In this paper, we propose a novel framework performing neural-logic reasoning to enable interpretability by visualizing the relational paths to tasks. Exploiting multi-hop reasoning, attention mechanism, and hierarchical reinforcement learning, our approach can solve large-sized complex problems like Montezuma’s Revenge, in contrast to other recent neuro-symbolic approaches. Compared to other black-box methods, our approach naturally operates with symbolic knowledge while achieving comparable performance and preserving interpretability. As future work, our framework can be extended to allow more expressive rules such as tree-like or junction-like rules [Yang and Song, 2020]. Such extensions could improve further the performance and the interpretability of NSRL. Another interesting and important research direction is to learn the predicates directly from high-dimensional inputs (e.g., images).

References

- Osbert Bastani, Yewen Pu, and Armando Solar-Lezama. Verifiable reinforcement learning via policy extraction. In *Proceedings of the 32nd International Conference on Neural Information Processing Systems*, pages 2499–2509, 2018.
- Youri Coppens, Kyriakos Efthymiadis, Tom Lenaerts, and Ann Nowé. Distilling deep reinforcement learning policies in soft decision trees. In *Proceedings of the IJCAI 2019 Workshop on Explainable Artificial Intelligence*, 2019.
- Andrew Cropper, Sebastijan Dumančić, and Stephen H Muggleton. Turning 30: New ideas in inductive logic programming. In *International Joint Conference on Artificial Intelligence (IJCAI)*, 2020.
- Rajarshi Das, Arvind Neelakantan, David Belanger, and Andrew McCallum. Chains of reasoning over entities, relations, and text using recurrent neural networks. *Conference of The European Chapter of The Association for Computational Linguistics*, 1:132–141, 2017.
- Honghua Dong, Jiayuan Mao, Tian Lin, Chong Wang, Li-hong Li, and Dengyong Zhou. Neural logic machines. *International Conference on Learning Representations*, 2019.
- R Evans and E Grefenstette. Learning explanatory rules from noisy data. *Journal of Artificial Intelligence Research*, 61(1):1–64, 2018.
- Matt Gardner and Tom Mitchell. Efficient and expressive knowledge base completion using subgraph feature extraction. In *Proceedings of the 2015 Conference on Empirical Methods in Natural Language Processing*, pages 1488–1498, 2015.
- Sam Greidanus, Anurag Koul, Jonathan Dodge, and Alan Fern. Visualizing and understanding atari agents. *International Conference On Machine Learning*, pages 1787–1796, 2018.
- Piyush Gupta, Nikaash Puri, Sukriti Verma, Dhruv Kayastha, Shripad Deshmukh, Balaji Krishnamurthy, and Sameer Singh. Explain your move: Understanding agent actions using focused feature saliency. *arXiv preprint arXiv:1912.12191*, 2019.
- Zhengyao Jiang and Shan Luo. Neural logic reinforcement learning. *International Conference on Machine Learning*, pages 3110–3119, 2019.
- Zoe Juozapaitis, Anurag Koul, Alan Fern, Martin Erwig, and Finale Doshi-Velez. Explainable reinforcement learning via reward decomposition. In *IJCAI/ECAI Workshop on Explainable Artificial Intelligence*, 2019.
- Tejas D. Kulkarni, Karthik Narasimhan, Ardavan Saeedi, and Josh Tenenbaum. Hierarchical deep reinforcement learning: Integrating temporal abstraction and intrinsic motivation. In Daniel D. Lee, Masashi Sugiyama, Ulrike von Luxburg, Isabelle Guyon, and Roman Garnett, editors, *NeurIPS*, pages 3675–3683, 2016.
- Ni Lao and William W Cohen. Relational retrieval using a combination of path-constrained random walks. *Machine Learning*, 81(1), 2010.
- Zachary C Lipton. The mythos of model interpretability. *arXiv preprint arXiv:1606.03490*, 2016.
- Daoming Lyu, Fangkai Yang, Bo Liu, and Steven Gustafson. Sdrl: Interpretable and data-efficient deep reinforcement learning leveraging symbolic planning. In *AAAI*, volume 33, pages 2970–2977, 2019.
- Prashan Madumal, Tim Miller, Liz Sonenberg, and Frank Vetere. Explainable reinforcement learning through a causal lens. volume 34, pages 2493–2500, 2020.
- Volodymyr Mnih, Koray Kavukcuoglu, David Silver, Andrei A Rusu, Joel Veness, Marc G Bellemare, Alex Graves, Martin Riedmiller, Andreas K Fidjeland, Georg Ostrovski, et al. Human-level control through deep reinforcement learning. *Nature*, 518(7540):529–533, 2015.
- Vinod Nair and Geoffrey E Hinton. Rectified linear units improve restricted boltzmann machines. In *Proceedings of the 27th International Conference on International Conference on Machine Learning*, pages 807–814, 2010.
- Ali Payani and Faramarz Fekri. Incorporating relational background knowledge into reinforcement learning via differentiable inductive logic programming. *arXiv preprint arXiv:2003.10386*, 2020.
- Tom Schaul, John Quan, Ioannis Antonoglou, and David Silver. Prioritized experience replay. *arXiv preprint arXiv:1511.05952*, 2015.
- John Schulman, Philipp Moritz, Sergey Levine, Michael Jordan, and Pieter Abbeel. High-dimensional continuous control using generalized advantage estimation. *arXiv preprint arXiv:1506.02438*, 2015.
- John Schulman, Filip Wolski, Prafulla Dhariwal, Alec Radford, and Oleg Klimov. Proximal policy optimization algorithms. *arXiv preprint arXiv:1707.06347*, 2017.
- Pedro Sequeira and Melinda Gervasio. Interestingness elements for explainable reinforcement learning: Understanding agents’ capabilities and limitations. *Artificial Intelligence*, 288:103367, 2020.
- Shaoyun Shi, Hanxiong Chen, Weizhi Ma, Jiaxin Mao, Min Zhang, and Yongfeng Zhang. Neural logic reasoning. In *Proceedings of the 29th ACM International Conference*

- on *Information & Knowledge Management*, pages 1365–1374, 2020a.
- Wenjie Shi, Zhuoyuan Wang, Shiji Song, and Gao Huang. Self-supervised discovering of causal features: Towards interpretable reinforcement learning. *arXiv preprint arXiv:2003.07069*, 2020b.
- David Silver, Julian Schrittwieser, Karen Simonyan, Ioannis Antonoglou, Aja Huang, Arthur Guez, Thomas Hubert, Lucas Baker, Matthew Lai, Adrian Bolton, et al. Mastering the game of go without human knowledge. *Nature*, 550(7676):354–359, 2017.
- Nicholay Topin and Manuela Veloso. Generation of policy-level explanations for reinforcement learning. *Proceedings of the AAAI Conference on Artificial Intelligence*, 33(01):2514–2521, 2019.
- Hado Van Hasselt, Arthur Guez, and David Silver. Deep reinforcement learning with double q-learning. In *Proceedings of the AAAI Conference on Artificial Intelligence*, volume 30, 2016.
- Ashish Vaswani, Noam Shazeer, Niki Parmar, Jakob Uszkoreit, Llion Jones, Aidan N Gomez, Łukasz Kaiser, and Illia Polosukhin. Attention is all you need. In *Proceedings of the 31st International Conference on Neural Information Processing Systems*, pages 6000–6010, 2017.
- A Verma. Imitation-projected programmatic reinforcement learning. *Advances in neural information processing systems*, 32, 2019.
- Abhinav Verma, Vijayaraghavan Murali, Rishabh Singh, Pushmeet Kohli, and Swarat Chaudhuri. Programmatically interpretable reinforcement learning. In *International Conference on Machine Learning*, pages 5045–5054. PMLR, 2018.
- Ronald J Williams. Simple statistical gradient-following algorithms for connectionist reinforcement learning. *Machine learning*, 8(3-4):229–256, 1992.
- Fan Yang, Zhilin Yang, and William W Cohen. Differentiable learning of logical rules for knowledge base reasoning. In *Advances in Neural Information Processing Systems*, pages 2316–2325, 2017.
- Yuan Yang and Le Song. Learn to explain efficiently via neural logic inductive learning. *International Conference on Learning Representation*, 2020.
- Tom Zahavy, Nir Ben-Zrihem, and Shie Mannor. Graying the black box: Understanding dqns. In Maria-Florina Balcan and Kilian Q. Weinberger, editors, *ICML*, volume 48, pages 1899–1908, 2016.
- Vinicius Zambaldi, David Raposo, Adam Santoro, Victor Bapst, Yujia Li, Igor Babuschkin, Karl Tuyls, David Reichert, Timothy Lillicrap, Edward Lockhart, et al. Relational deep reinforcement learning. *arXiv preprint arXiv:1806.01830*, 2018.